Journal of Materials and Construction
ISSN 2734-9438
Website: www. jomc.vn

Recycled aluminum can fibers for concrete reinforcement: Standardized testing of compressive strength and static elastic modulus

Lam Thanh Quang Khai[1,*], **Do Nguyen Ngoc Ha**[1]

[1]Faculty of Civil Engineering, Mien Tay Construction University

KEYWORDS

Concrete
Recycling
Aluminum fibers
Compressive strength
Elastic modulus

ABSTRACT

This study examines the feasibility of repurposing post-consumer aluminum beverage-can scrap into macro-fibers for concrete reinforcement as a pathway toward more sustainable construction materials. Although aluminum offers low density, inherent corrosion resistance in many environments, and abundant waste streams, data on concrete reinforced with fibers cut from recycled cans remain limited. Cleaned cans were slit into strips of 100 × 10 × 1 mm and added at a 2% fiber volume fraction to a B15 concrete. Cube compressive strength was determined on 150 mm cubes in accordance with TCVN 3118:2022, and the static modulus of elasticity was measured on 150 × 300 mm cylinders following TCVN 5726:2022. Measured moduli were also compared with code-based predictions from ACI 318-19, AS 3600:2018, BS 8110-2:1985, and Eurocode 2 (EN 1992-1-1). Relative to the plain control, the aluminum fiber–reinforced concrete exhibited ~22% lower cube strength (20.6 → 16.1 MPa) and ~11% lower modulus (23.99 → 21.31 GPa). The absolute differences between measured and code-predicted moduli were 5.8% (ACI), 11.3% (AS), 12.6% (BS), and 27.1% (EC2), indicating that current equations are not calibrated for concrete reinforced with recycled aluminum-can fibers. Compared with steel-fiber concrete, aluminum fibers did not enhance compressive strength but may offer benefits in post-cracking toughness, corrosion performance, and circularity. Recycled aluminum-can fibers appear feasible for non-structural or weight-sensitive concrete applications. Future work should optimize fiber geometry and dosage, improve dispersion and constructability, and include standardized flexural tests (ASTM C1609, EN 14651) to quantify post-cracking behavior.

1. Introduction

Within the broader agenda of the circular economy and emissions mitigation for the construction sector, recycling aluminum beverage cans offers substantial energy savings—up to ~95 % relative to primary production—and is therefore a compelling pathway to upcycle can scrap into construction materials [1]. In the mechanics of materials domain, fiber-reinforced concrete (FRC) is routinely characterized in flexure using ASTM C1609 (load–deflection under third-point loading) and EN 14651 (load–CMOD on notched beams), while RILEM TC 162-TDF provides design recommendations, collectively underscoring the role of fibers in enhancing post-cracking toughness and crack control [2–4]. For aluminum strips/fibers used in concrete, experimental findings indicate that mechanical performance depends strongly on fiber geometry, volume fraction, and mixing/placing procedures; several configurations report improvements in flexural/impact indicators, whereas effects on compressive strength remain scattered [5–8].

At the mechanistic level, electrochemical interaction between aluminum and the alkaline cementitious pore solution can generate H_2 gas and induce porosity if uncontrolled; recent studies have analyzed gas-evolution kinetics and the influence of alkalinity on the stability of the native Al-oxide film [9–10]. In parallel, many structural codes still employ modulus-of-elasticity equations calibrated for plain (non-fibrous) concrete—e.g., ACI 318, EN 1992-1-1 (EC2), AS 3600, and BS 8110-2—raising questions about their direct applicability to recycled aluminum fiber-reinforced concrete [11–14]. Emerging research on aluminum–binder interactions suggests that surface modification and/or corrosion-inhibition strategies can mitigate adverse effects in ordinary Portland cement systems, or that alternative binders (e.g., magnesium potassium phosphate cement, MKPC) may be considered [15–17]. From a fundamental chemistry viewpoint, the kinetics of hydrogen evolution for Al reacting with NaOH/H_2O have been quantified, helping rationalize microstructural observations when Al contacts fresh concrete [18]. System-level assessments further emphasize the energy- and emission-reduction benefits of aluminum recycling, reinforcing the urgency of deploying recycled-aluminum solutions in construction materials.

Building on this context, the present study repurposes post-consumer can aluminum into thin ribbon-type macro-fibers (100 × 10 × 1 mm) dosed at V_f = 2 % in a B15 concrete. We measure cube compressive strength on 150-mm cubes in accordance with TCVN

*Corresponding author: Lamkhai@mtu.edu.vn
Received 10/11/2025, Revised 22/11/2025, Accepted 24/11/2025
Link DOI: https://doi.org/10.54772/jomc.v15i02.1179

3118:2022 and the static modulus of elasticity on 150 × 300 mm cylinders following TCVN 5726:2022. The measured modulus E_c is benchmarked against predictions from ACI 318, EC2, AS 3600, and BS 8110-2, quantifying prediction–experiment discrepancies using the same specimen geometries to maintain consistency.

2. Materials and Methods

2.1. Materials

Materials and Curing: A Portland blended cement (PCB40 per TCVN) was used. Natural sand and crushed-stone coarse aggregate complied with the relevant TCVN requirements on physical–chemical properties and grading. Mixing water and curing procedures followed TCVN 3105:2022, with specimens moist-cured under standard conditions for 28 days.

Recycled Aluminum Fibers: Post-consumer beverage-can aluminum was cleaned and slit into ribbon-type macro-fibers with an average geometry of ≈100 × 10 × 1 mm (length × width × thickness). Fibers were dosed at a volume fraction V_f = 2 %. To keep mixture volume constant, the fiber volume replaced an equivalent volume of fine aggregate (sand). Preparation and geometry are illustrated in Fig. 1.

Fig 1. Recycled Aluminum Fibers.

2.2. Mix design and specimen-specific volumetric conversion

The base mix for a B15 concrete per cubic meter comprised sand 653.96 kg, coarse aggregate 1,419.53 kg, water 239.03 kg, and cement 433.67 kg (w/c ≈ 0.55). For specimen-level batching, scaling by volume yielded the following control (plain) quantities:

- 150×150×150 mm cubes (V ≈ 10 liters): sand 6.62 kg, coarse aggregate 14.38 kg, water 2.43 kg, cement 4.39 kg.
- 150×300 mm cylinders (V ≈ 16 liters): sand 10.40 kg, coarse aggregate 22.60 kg, water 3.82 kg, cement 6.90 kg.
- Aluminum fiber–reinforced concrete with V_f = 2 % (by volume): for V ≈ 10 liters, the fiber mass is ≈ 0.133 kg; for V ≈ 16 liters, ≈ 0.208 kg.

Water content was initially kept constant, with high-range water-reducing admixture (if used) dosed to restore the target slump of 6 ± 2 cm, acknowledging the typical slump loss associated with macro-fibers.

2.3. Mixing, casting, and curing

Aggregates were dry-mixed while gradually feeding the recycled aluminum fibers to minimize balling. Cement was then added, followed by the pre-blended mixing water/high-range water-reducing admixture solution. Mixing continued until a uniform, fiber-dispersed consistency was achieved (≈2–3 min after full water addition).

Specimens were placed in lifts and consolidated using an internal vibrator operating at ≈7,200 vpm (vibrations per minute); the vibrator head was kept clear of the mold base, and each insertion penetrated 25–50 mm into the underlying lift. The surface was struck off and finished flush.

Curing followed TCVN 3105:2022: specimens were moist-cured for 28 days under standard conditions (27 ± 2 °C; 95 ± 5 % relative humidity).

2.4. Test matrix and specimen counts

Compressive strength (TCVN 3118:2022): For each mix, n = 3 cubes of 150 × 150 × 150 mm were tested for the plain control and n = 3 for the aluminum fiber–reinforced concrete. Acceptance followed the TCVN criterion that no individual result may deviate by more than ±15 % from the companion results; otherwise, outlier handling/retesting was performed per the standard.

Static modulus of elasticity (TCVN 5726:2022): For each mix, n = 3 cylinders of 150 × 300 mm (L/D = 2) were tested to determine E_c. The choice L/D = 2 ensures geometric compatibility when benchmarking measured moduli against code equations in ACI 318, EC2, AS 3600, and BS 8110-2.

For contextual comparison, 150-mm cubes of B22.5 concrete reinforced with steel fibers at 1–3 % (by volume) and fiber lengths of 30–50 mm were included as a reference [19].

2.5. Compressive strength test (TCVN 3118:2022)

Tests were performed on a calibrated compression testing machine compliant with TCVN requirements (e.g., an ELE frame of ~1500 kN nominal capacity). Specimens were centered between hardened, spherical-seated platens; bearing faces were prepared in accordance with the standard (capped or ground as required). Loading was applied monotonically at a constant stress rate of ≈0.6 MPa/s until failure.

The cube compressive strength for each specimen was computed

as (equation 1):

$$R = \alpha \times \frac{P}{A} \quad (1)$$

where P is the failure load in newtons (N), A is the loaded area in mm^2, and α is a shape factor (α = 1.0 for 150-mm cubes). An individual result was considered out-of-tolerance if it deviated by more than ±15 % from the set mean (or per the specific outlier rule in TCVN 3118:2022); such cases were handled/retested in accordance with the standard.

2.6. Static modulus of elasticity (TCVN 5726:2022)

Instrumentation: Cylinders (150 × 300 mm, L/D = 2) were equipped with a clip-on extensometer or frame-mounted gauge having a resolution/accuracy ≤ 0.002 mm. Two opposed gauges were mounted along a gauge length L_g (e.g., 200 mm) centered on the specimen midheight; axial strain was taken as the average of the two gauge readings. Displacement transducers were zeroed under a small seating load.

The secant modulus was computed as (equation 2),

$$E = \frac{\sigma_1}{\varepsilon_{1y}}, \quad \sigma_1 = \frac{P1}{A}, \quad P_1 = 0{,}3 \times P_e \quad (2)$$

where P_e is the ultimate (failure) load in Newtons (N), A is the loaded area in (mm^2), For each set (n=3), the set mean was reported. If any individual result deviated by more than ±15 % from the companion results, the extreme outlier (highest or lowest) was discarded and the mean was recomputed in accordance with the standard.

2.7. Code-based prediction of elastic modulus

To benchmark against test data, code equations were evaluated in SI units with a consistent strength definition and, where required, a cube→cylinder mapping.

ACI 318-19 [11], equation 3:

$$E_c = 57000 \times \sqrt{f'_c} \text{ (Psi) or: } E_c = 4700 \times \sqrt{f'_c} \text{ (Mpa)} \quad (3)$$

where: f'_c is cylinder strength (MPa)

Eurocode 2 (EN 1992-1-1) [12], equation 4:

$$E_c = 22 \times 10^3 \times \left(\frac{f_{cm}}{10}\right)^{0.3} \text{ (MPa)} \quad (4)$$

where: f_{cm}: is the mean cylinder strength (MPa)

AS 3600:2018 [13], equation 5 and equation 6:

$$E_c = 0.043 {p_c}^{1.5} \sqrt{f_{cm}} \text{ (MPa) with } f_{cm} \leq 40 \text{ MPa} \quad (5)$$

$$E_c = 0.024 {p_c}^{1.5} \sqrt{f_{cmi}} + 0.12) \text{ (MPa) with } f_{cm} > 40 \text{ MPa} \quad (6)$$

with ρ_c in kg/m^3, and notes an indicative ±20 % scatter.

BS 8110-2:1985 [14], equation 7:

$$E_c = 20 + 0.2\, f_{cu} \text{ (GPa)} \quad (7)$$

3. Results and discussions

3.1. Compressive behavior of aluminum fiber–reinforced concrete (Al-FRC)

At 28 days, concrete with 2 % (by volume) recycled aluminum fibers (≈100 × 10 × 1 mm) exhibited a ~22 % reduction in cube compressive strength, decreasing from 20.6 MPa to 16.1 MPa relative to the B15 plain control. This reduction is plausibly associated with (i) increased entrapped/entrained voids and imperfect dispersion caused by the ribbon geometry and suboptimal fiber orientation at V_f = 2 %, and (ii) potential aluminum–alkaline pore solution interactions that can evolve H_2 when surface conditioning is inadequate. These mechanisms are consistent with the observed macro-voids and heterogeneous fiber alignment in the tested mixes (Fig. 2).

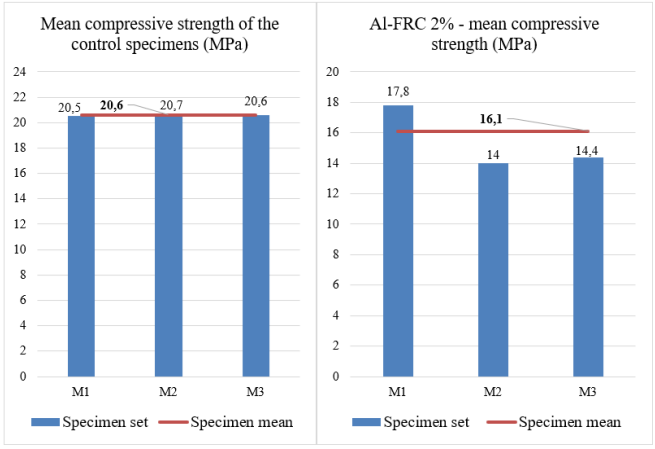

Fig.2. Chart of mean compressive strength for the concrete specimen types.

Static secant modulus of elasticity (TCVN 5726:2022): The control concrete exhibited a static secant modulus of 23.99 GPa, whereas the Al-FRC (V_f = 2 %) reached 21.31 GPa, corresponding to an ≈11.2 % reduction. These results indicate a lower elastic modulus for the aluminum-fiber system relative to the plain mix (Fig. 3).

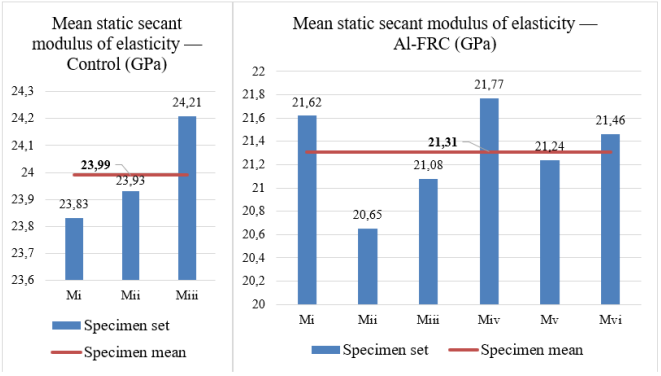

Fig.3. Chart of the mean elastic modulus across the concrete specimen types.

The calculated elastic modulus of the two concrete types according to selected international standards is presented in Table 1.

Table 1. Elastic modulus of the two concrete types according to selected standards.

Standards	Equation	Elastic modulus (GPa)			Percent difference %	
		with standard	experimental results TCVN 5726:2022			
			control specimens	2 % Al-FRC		
AS 3600:2018	$E_c = 0{,}043 p_c^{1,5}\sqrt{f_{cm}} = 0{,}043 \times 24^{1,5}\sqrt{22}$ $(p = 2400\ kg/m^3)$	23,71	23,99	21,31	1,17	11,26
BS 8110-2: 1985	$E_c = 20 + 0{,}2\ f_{cu} = 20 + 0{,}2 \times 20$	24			0,04	12,62
EN 1992-1-1: 2004	$E_c = 22.10^3.\left(\frac{f_{cm}}{10}\right)^{0,3} = 22.10^3.\left(\frac{20}{10}\right)^{0,3}$	27,09			12,9	27,12
ACI 318-19	$E_c = 4700 \times \sqrt{f'_c} = 4700 \times \sqrt{23}$	22,54			6,04	5,77

Code-to-test comparison: The percent differences between the measured and code-predicted elastic modulus were approximately 5.8 % (ACI 318-19), 11.3 % (AS 3600:2018), 12.6 % (BS 8110-2:1985), and 27.1 % (EC2) (Fig. 4). Accordingly, the agreement ranks ACI > AS ≈ BS > EC2, with EC2 systematically overestimating the measured values, shown in Fig.4

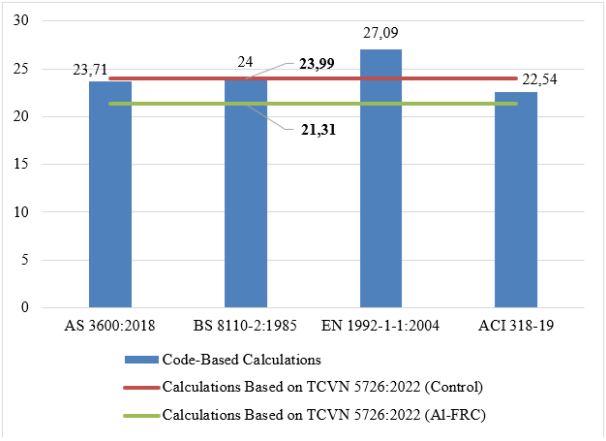

Fig.4. Elastic modulus from standards vs. Experiment.

Normalized comparison: Relative to their respective plain controls, the Al-FRC (V_f = 2 %) exhibited a −22 % change in cube compressive strength and a −11 % change in the static secant modulus E_c. By contrast, the SFRC (V_f = 2 %, $l \approx$ 30 mm) showed a +18 % gain in strength with negligible change in E_c. These trends highlight the superior chemo-mechanical efficiency of steel fibers in enhancing load-bearing capacity, whereas aluminum ribbons are not mechanically optimal at the tested geometry/dosage but may be attractive for weight-sensitive or thermally conductive applications. To improve Al-FRC performance, we recommend alkali-resistant surface treatments (e.g., conversion/anodic coatings or thin polymer coatings), mix optimization to minimize entrapped air (HRWR/VMA, dispersion protocol), and hybrid fiber systems (aluminum–steel or aluminum–polymer) to leverage complementary benefits.

3.2. Benchmarking and evaluating elastic modulus against standards

The measured static secant modulus was benchmarked against domestic and international provisions to quantify prediction error and assess model reliability. TCVN 3118:2022 uses 150 × 150 × 150 mm cubes, which are simple and repeatable under local laboratory conditions; however, international comparisons require a consistent mapping from cube strength (f_{cu}) to cylinder strength ($f'c$). TCVN 5726:2022 determines the static modulus on 150 × 300 mm cylinders (L/D = 2), providing strong geometric compatibility with code equations and specifying reference loading with $P_1 = 0.3P_u$, which enhances accuracy and repeatability. Relative to ASTM C469, the TCVN procedure yields comparable E_c values, differing mainly in how the strain origin is defined; consequently, cross-standard comparability is preserved.

Overall, the agreement with experiments ranked ACI (best) → AS ≈ BS (intermediate) → EC2 (overestimation). This pattern indicates that plain-concrete modulus equations in current codes do not fully capture the effects of recycled aluminum fibers. A pragmatic remedy is to introduce an Al-FRC calibration factor k_{Al} (multiplying the code-predicted E_c) or to re-fit the coefficient/exponent for the strength term using Al-FRC datasets, thereby reducing systematic bias.

4. Conclusions

This study assessed the feasibility of repurposing post-consumer aluminum beverage cans into ribbon-type macro-fibers for concrete reinforcement (Al-FRC) and benchmarked the measured static secant modulus of elasticity against widely used code equations. Tests followed TCVN 3118:2022 (150-mm cubes) and TCVN 5726:2022 (150×300-mm cylinders, L/D = 2).

1. Mechanical performance at 28 days:

- Compressive strength: Al-FRC at $V_f = 2$ % ($\approx 100 \times 10 \times 1$ mm ribbons) achieved 16.1 MPa, i.e., -22 % vs. the plain B15 control (20.6 MPa), but still satisfies the target grade in absolute terms. The reduction is plausibly associated with increased voids/heterogeneous orientation at high V_f and potential Al–alkali interactions when surface conditioning is insufficient.

- Elastic modulus: The control exhibited $E_c = 23.99$ GPa and Al-FRC $E_c = 21.31$ GPa, a -11.2 % change, indicating a lower short-term stiffness for Al-FRC at the tested geometry/dosage.

2. Code-to-test comparison (predicted vs. measured E_c):

Using consistent SI units and cube→cylinder mapping where required, were ACI 318-19 $\approx +5.8$ %, AS 3600:2018 $\approx +11.3$ %, BS 8110-2:1985 $\approx +12.6$ %, and EC2 $\approx +27.1$ %. Agreement ranks ACI $>$ AS $\approx$ BS $>$ EC2, with EC2 systematically overestimating E_c

3. Sustainability and use-cases:

Recycling can-aluminum into fibers supports circular-economy goals. Given the measured stiffness/strength trends, non-structural or weight-sensitive applications are presently the most suitable for Al-FRC at $V_f = 2$ % with the tested ribbon geometry.

4. Recommendations for improving Al-FRC:

- Fiber & mix engineering: optimize ribbon geometry (reduce thickness/width, increase aspect ratio prudently), explore lower V_f with better dispersion, and apply HRWR/VMA to control slump/air.

- Surface conditioning: employ alkali-resistant/coated aluminum (conversion/ anodic/polymeric films) to mitigate early Al–alkali reactions and gas evolution.

Acknowledgments

The research reported in this paper is part of the student research project. The authors gratefully acknowledge the support of MTU for providing the facilities and funding that made this work possible.

References

[1]. International Aluminium Institute, “Aluminium recycling and climate: energy and emissions benefits,” Report, 2024.

[2]. ASTM International, ASTM C1609/C1609M-12**:** *Standard Test Method for Flexural Performance of Fiber-Reinforced Concrete (Using Beam With Third-Point Loading)*, 2012.

[3]. CEN, EN 14651:2005: *Test method for metallic fibre concrete—Measuring the flexural tensile strength (LOP & residual)*, 2005.

[4]. σ–ε design method,” *Materials and Structures*, 36, pp. 560–567, 2003, DOI: 10.1007/BF02480834

[5]. Y. K. Sabapathy, S. Sabarish, C.N.A Nithish, S.M. Ramasamy, G. Krishna, “Experimental study on strength properties of aluminium fibre reinforced concrete,” *Journal of King Saud University – Engineering Sciences*, 33(1), pp. 23–29, 2021, DOI: 10.1016/j.jksues.2019.12.004

[6]. S. P. Muñoz Perez, J. M. Garcia Chumacero, S. Charca Mamani, and L. I. Villena Zapata, “Influence of the secondary aluminum chip on the physical and mechanical properties of concrete,” *Innovative Infrastructure Solutions*, 8, art. 45, 2022, DOI: 10.1007/s41062-022-01015-3

[7]. C. D. Agor, E. M. Mbadike, and G. U. Alaneme, “Evaluation of sisal fiber and aluminum waste concrete blend for sustainable construction using adaptive neuro-fuzzy inference system,” *Scientific Reports*, 13(1), art. 2814, 2023, DOI: 10.1038/s41598-023-30008-0

[8]. Elseknidy, M. H., Salmiaton, A., Nor Shafizah, I., & Saad, A. H. “A Study on Mechanical Properties of Concrete Incorporating Aluminum Dross, Fly Ash, and Quarry Dust”. *Sustainability*, 12(21), 9230, 2020. DOI: 10.3390/su12219230

[9]. Abd El Haleem, S.M., El Wanees, S.A. & Farouk, A. Hydrogen Production on Aluminum in Alkaline Media. *Prot Met Phys Chem Surf*, 57, 906–916 (2021). DOI: 10.1134/S2070205121050099

[10]. Mohamed Esaker, Georgia E. Thermou, Luis Neves, “Impact resistance of concrete and fibre-reinforced concrete: A review,” *International Journal of Impact Engineering*, 180, 104722, 2023, DOI: 10.1016/j.ijimpeng.2023.104722

[11]. ACI Committee 318, ACI 318-19**:** *Building Code Requirements for Structural Concrete*, 2019.

[12]. EN 1992-1-1:2004 (Eurocode 2)**:** *Design of Concrete Structures—General Rules and Rules for Buildings*, 2004.

[13]. Australian strandard, AS 3600:2018**:** *Concrete Structures*, 2018.

[14]. British Standards Institution, BS 8110-2:1985: *Structural Use of Concrete—Part 2: Code of Practice for Special Circumstances*, 1985.

[15]. C. Fernández-García, P. Padilla-Encinas, R. Fernández, M.C. Alonso, “Interaction of aluminum alloys with MKPC and Portland-based cements on the metal–matrix interface,” *Applied Geochemistry*, 172, 106105, 2024, DOI: 10.1016/j.apgeochem.2024.106105

[16]. H. Kinoshita, P. Swift, C. Utton, B. Carro-Mateo, G. Marchand, N. Collier, N. Milestone, “Corrosion of aluminium metal in OPC- and CAC-based cement matrices,” *Cement and Concrete Research*, 50, pp. 11–18, 2013, DOI: 10.1016/j.cemconres.2013.03.016

[17]. Geng, H., Wei, Q., Ma, H., & Li, Q. “Inhibition Mechanism of Corrosion of Aluminium Alloy in Ordinary Portland Cement Paste by Polyaluminium Sulphate”. *Ceramics*, 8(1), 27. 2025. DO: 10.3390/ceramics8010027

[18]. V. Testa, M. Gerardi, L. Zannini, M. Romagnoli, P.E. Santangelo, “Hydrogen production from aluminum reaction with NaOH/H_2O solution: Experiments and insight into reaction kinetics,” *International Journal of Hydrogen Energy*, 83, pp. 589-603, 2024, DOI: 10.1016/j.ijhydene.2024.08.152

[19]. T. Q. K. Lam, Q. K. Cao, H. H. Dao, T. T. Le, M. T. Vo, and T. K. Nguyen, “Effect of length and percentage of dispersed steel wire on compressive strength of concrete,” *Lecture Notes in Civil Engineering*, 456, pp. 391–403, 2024, DOI: 10.1007/978-981-99-9458-8_37